

Chapter 13

Precision Agriculture Technologies for Management of Plant Diseases



Siva K. Balasundram, Kamlesh Golhani, Redmond R. Shamshiri,
and Ganesan Vadamalai

Abstract Plant diseases contribute 10–16% losses in global harvests each year, costing an estimated US\$ 220 billion. Abundant use of chemicals such as bactericides, fungicides, and nematicides to control plant diseases are causing adverse effects to many agroecosystems. Precision plant protection offers a non-destructive means of managing plant diseases based on the concept of spatio-temporal variability. Global Navigation Satellite System (GNSS) and Geographic Information System (GIS) allow for assessment of field heterogeneity due to disease problems and can enable site-specific intervention. Similarly, hyperspectral remote sensing is a cutting-edge spectral approach for plant diseases detection. The main aim of precision plant protection is to significantly reduce the injudicious use of chemical inputs and hence the adverse impact of chemicals to the environment. This chapter provides some insights into the deployment of site- and time-specific approaches to manage plant disease problems in a balanced and optimized manner.

Keywords Precision agriculture · Global positioning systems · Geographic information systems · Remote sensing · Spectroradiometer

S. K. Balasundram (✉) · K. Golhani · R. R. Shamshiri
Department of Agriculture Technology, Universiti Putra Malaysia (UPM),
Serdang, Selangor, Malaysia

G. Vadamalai
Department of Plant Protection, Universiti Putra Malaysia (UPM),
Serdang, Selangor, Malaysia

© Springer Nature Switzerland AG 2020

I. Ul Haq, S. Ijaz (eds.), *Plant Disease Management Strategies for Sustainable Agriculture through Traditional and Modern Approaches*, Sustainability in Plant and Crop Protection 13, https://doi.org/10.1007/978-3-030-35955-3_13

259

13.1 Introduction

13.1.1 *Plant Disease Management*

Crop stress represents a major challenge in agricultural production. Stress sources are classified into two categories: biotic and abiotic. Biotic stresses are caused by diseases (Carter and Knapp 2001), insect pests (Riedell et al. 2000) and weeds (Pinter et al. 2003), while abiotic stresses are caused by physical factors such as water deficit (Steele et al. 2008), salinity overload (Pinter et al. 2003), and nutrient deficiency (Blackmer et al. 1995). Particularly, plant diseases result in changes in crop physiology (transpiration, photosynthesis), morphology (tissue shape or color) and crop density (West et al. 2010). Changes in host plants are also caused by hypersensitive reactions (Chaerle 2004) and cell wall degradation (Blackburn 2007).

At present, plant diseases represent a major threat to the global economy. Severe economic losses have been incurred in the agriculture industry due to diseases. Therefore, effective disease monitoring and early detection system should be facilitated to reduce their incidence and spread (Martinelli et al. 2014). It has been reported that many developed countries have established disease surveillance system. In developing countries, however, where dense populations reside and extensive agricultural operations take place, disease surveillance systems are lacking (Lemon et al. 2007). Precision agriculture could be a very useful and effective approach to enable disease surveillance at the field scale.

13.1.2 *Precision Agriculture vis-à-vis Plant Protection*

Precision agriculture comprises management strategies that use information technology to process high resolution spatial and temporal data related to crop production. From tillage to harvesting, precision agriculture provides different packages of operations to reduce inputs, increase profits, and protect the environment. Recently, under the umbrella of precision agriculture, a new branch popularly known as “precision plant protection” has emerged. Precision plant protection means taking the right action in the right place at the right time, to protect plants from biotic and abiotic stresses. Precision plant protection comprises disease management strategies based on precision agriculture tools. Remote sensing, Geographic Information System (GIS) and Global Navigation Satellite System (GNSS), Unmanned Aerial Vehicle (UAV) and machine learning techniques such as Artificial Neural Network (ANN), with Partial Least Square (PLS) are the major drivers being applied.

Oerke et al. (2010) showed that the strategies for precision plant protection should be planned on the basis of information obtained from the previous crops. Only then, a proper precision plant protection program can be implemented. Over the last decade, most studies focused on the application of remote sensing for early disease detection (Lee et al. 2010). Some examples include diseases caused by fungi

(West et al. 2010), viruses (Grisham et al. 2010; Krezhova et al. 2015) and viroids (Beltrán-Peña et al. 2014; Golhani et al. 2017a, b, 2019a; Selvaraja et al. 2013). Rumpf et al. (2010) highlighted the use of different data mining techniques with hyperspectral data for plant disease detection.

13.2 Orange Spotting Disease in Malaysia

Orange Spotting (OS) is an emerging disease of oil palm (*Elaeis guineensis* Jacq.; Arecaceae) in Malaysia. Coconut cadang-cadang viroid (CCCVd) is the causal agent of OS disease. CCCVd is one of the known species of viroids, which thus far have only been found in plants. They are single-stranded, low molecular weight, circular RNAs between 246 and 401 nucleotides that lack a protective protein coat (Diener 1999). Recent reports indicate that OS disease can result in an epidemic that could bring significant economic losses to oil palm production in Malaysia. In 2006, for the first time, three CCCVd variants (OP₂₉₇, OP₂₉₃, and OP₂₇₀) were reported in an asymptomatic oil palm in Malaysia. This was the first incident outside the Philippines in a species other than coconut palm (Vadamalai et al. 2006). Then, Wu et al. (2013) reported the first incident of a variant of CCCVd (OP₂₄₆) with clear orange color spots. In a recent investigation, an oil palm variant (OP₂₉₃) showed low accumulation of viroid load with no symptoms, 1 year after inoculation (Thanarajoo 2014).

Selvaraja et al. (2013) reported OS disease has similar foliar symptoms to that of potassium deficiency in oil palm. Symptomatic separability between OS disease and potassium deficiency is also very difficult to achieve via visual assessment. It proves that symptom expression is not a necessary outcome of CCCVd infection. It is challenging to scout for healthy palms from the diseased palms due to the lack of visible symptoms. It is believed that the use of hyperspectral sensor (spectroradiometer) can serve as a useful tool for preliminary screening of CCCVd infected seedlings, at the nursery stage. Therefore, it is important to identify OS disease at an early stage, most preferably at the leaf scale (nursery stage). The current approach of remote sensing can serve as a useful tool for preliminary screening of CCCVd infected seedlings.

Real-time detection of OS disease has become possible now using a spectroradiometer. Existing molecular marker techniques typically take a longer time (3–6 months), from sampling to laboratory analysis, for detection of CCCVd infection. Instead, precision plant protection may provide rapid and non-invasive detection of OS disease. Recently, Golhani et al. (Golhani et al. 2017a, b; 2019a, b) used an Analytical Spectral Device (ASD) spectroradiometer for non-invasive detection of OS disease in oil palm. In this research, oil palm seedlings were inoculated with a CCCVd oil palm variant (OP₂₄₆). The research was designed to observe the spectral changes between CCCVd-inoculated and healthy oil palm seedlings followed by the development of spectral signatures, selection of red edge wavebands, selection of red edge indices and development of an Orange Spotting Disease Index (OSDI) using red edge parameters.

13.3 Objectives

The main objective of this chapter is to discuss major drivers of precision agriculture in the context of precision plant protection. This chapter describes hyperspectral remote sensing in general and Visible/Near-infrared (VNIR) spectroscopy and Spectral Disease Index (SDI) in particular. The advantages of UAV, GIS and GNSS are also discussed. Few machine learning techniques are also reviewed. In addition, a successful case study on OS disease detection comprising the use of remote sensing and machine learning techniques is reported.

13.4 Major Drivers in Precision Plant Protection

13.4.1 Remote Sensing

In order to efficiently apply remote sensing in precision plant protection, it is very important to understand the fundamental interaction of radiant energy with the earth surface (Huete 1989). The radiant energy (electromagnetic radiation) propagates through the atmosphere to the earth surface in the form of electromagnetic waves. These waves are well distributed across the electromagnetic spectrum comprising several spectral regions, viz. ultraviolet, blue, green, red, red edge and Near-infrared (NIR) (Fig. 13.1). The electromagnetic radiation interacts with the atmosphere in different ways via absorption, transmission, diffusion, scattering, and reflection. In this process, approximately 40% of the solar flux is received by the earth surface (Lacis and Hansen 1974).

The spectral composition of solar flux interacting with the earth surface provides information about the physical properties of soil, water, and vegetation. In vegetation (plant leaf and canopy), the reflectance from radiation results in diffuse and specular characteristics. Spectral diffusion takes place due to multiple scattering,

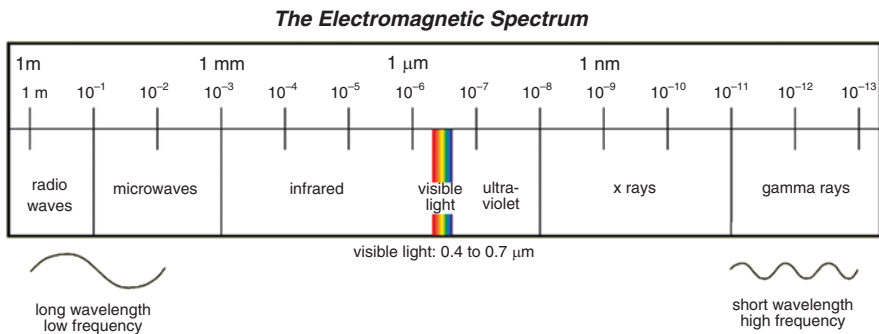


Fig. 13.1 The electromagnetic spectrum showing different segments of the spectrum comprising γ rays, X rays, ultraviolet, visible light, infrared, microwaves, and radio waves

depending on the different physical and structural design of the leaves. The topography of the cuticular wax and hair at the leaf surface affects specular characteristics of leaf reflectance. In remote sensing, spectral signatures are developed from leaf reflectance, which is often found to be sensitive to these changes. Light is scattered in all directions when interacting with unhealthy plant tissue, while the light is scattered in a diffused manner when interacting with healthy tissues, next to small symptomatic tissue present in the epidermis layer. Thomas et al. (2017) has recently studied plant-pathogen interaction using hyperspectral imaging reflectance and transmission measurements.

The measurement of reflectance has a significant role in detecting crop diseases as well as in quantifying the complex spatio-temporal dynamics of plant-pathogen interactions. Mahlein (2010) investigated foliar sugar beet diseases (*Cercospora* leaf spot, sugar beet rust, and powdery mildew) at the canopy and leaf scales using spectral signatures derived from hyperspectral sensors. The term “hyperspectral” refers to the use of hundred over contiguous narrow spectral bands. Hyperspectral sensors can be either active or passive. The sensor system equipped with its own source of radiation is called an active sensor, while sensors that depend on solar radiation are called passive sensors. Thus, the basic mechanism of remote sensing completely depends on the type of sensors (active or passive) being employed (Schellber et al. 2008).

13.4.2 Hyperspectral Remote Sensing

Hyperspectral remote sensing is also known as reflectance spectroscopy. Hyperspectral wavebands measure the reflectance from the leaf surface. On the basis of the percentage of reflectance of wavebands, different types of stress such as diseases, nutrient deficiency, and water scarcity can be differentiated at their corresponding spectral regions. Clevers et al. (2004) reported that leaf pigments dominate in the visible region (400–700 nm), while cell structure and leaf water contents dominate in the NIR (700–1000 nm) and Short-wave infrared (SWIR, 1000–2500 nm) regions, respectively. Changes in reflectance characteristics have been observed due to alterations in plant biochemistry and cellular composition of leaves. Unhealthy vegetation (senescent and stressed) has more reflection in the red region and lower reflectance in the NIR region (Li et al. 2005). In a landmark study, Knipling (1970) stated that low reflectance in the NIR region has been often associated with an advanced stage of disease attack, where the breakdown of leaf cells has taken place.

A practical hyperspectral sensor is the hand-held variant (called a spectroradiometer), which is available within a spectral range of 400–1100 nm (Visible/NIR or VNIR) and 400–2500 nm (Visible-NIR-SWIR). Slonecker (2011) recommends a multiscale spectroradiometer for laboratory-to-field scale experiments. Hand-held spectroradiometers can be used repeatedly in order to understand changes in spectral reflectance of plants. They are also called non-invasive crop sensors and

classified into imaging and non-imaging sensors, depending on their detection specifications. These sensors are primarily used for real-time stress detection.

According to Kuska and Mahlein (2018), hyperspectral sensors are potentially powerful tools in protecting crops against diseases. Hyperspectral sensors can facilitate a proximate and objective detection. Thomas et al. (2018) mentioned that hyperspectral sensors can play an important role for measuring pathogen-induced changes. They showed that hyperspectral sensors are practically diagnostic as well as valuable for disease investigation at different scales, from the tissue to the canopy level. Several recent studies have included early disease detection using hyperspectral imaging sensors (Mahlein 2016), disease forecasting from meteorological parameters (Grinn-Gofroń et al. 2019), disease warning (Gillespie and Sentelhas 2008), and estimation of disease stages using the Spectral Disease Index (SDI) (Ashourloo et al. 2016).

13.4.3 Visible/Near-Infrared (VNIR) Spectroscopy

The VNIR region is being widely explored in the field of precision plant protection. As an effort to increase the effectiveness of the VNIR region for studying plant diseases, different wavebands within this range have been examined. Ayala-Silva and Beyl (2005) described an unambiguous relationship between VNIR region and green parts of the plants. The maximum absorption was found in the blue (400–500 nm) and red (600–700 nm) regions via chlorophyll content, while maximum reflection was found in NIR region due to scattering in leaf mesophyll. VNIR spectra typically characterize the baseband frequency range of organic compounds, therefore they give potentially pertinent and inherent information about an object (Zhao 2012). Several recent studies (Ashourloo et al. 2016; Mahlein 2016; Rumpf et al. 2009) have explained the importance of the VNIR range in discriminating diseased plants.

Also, there is evidence of qualitative and quantitative changes of chlorophyll content in the course of plant growth, coupled with biotic and abiotic stresses. Merzlyak et al. (2003) developed algorithms for pigment analysis within the VNIR region. They showed that two spectral wavebands (550 nm and 700 nm) were more sensitive to chlorophyll content. According to Chappelle et al. (1992), chlorophyll absorption is reduced when plant growth is under stress due to the effect of biostressors. Carter and Miller (1994) demonstrated the importance of spectral wavebands and spectral ratios within 690–700 nm, which can provide early detection of stress-induced chlorosis.

13.4.4 Spectral Disease Index (SDI)

An SDI is developed from a combination of disease sensitive hyperspectral wavebands represented as a waveband ratio (Golhani et al. 2018). The SDI has the potential to discriminate and differentiate between diseased and healthy plants. Development of SDI comprises different methods of algebraic or mathematical analyses such as normalizing, differentiation, summation, and linear combinations. The preferred methods for development of SDI are continuum-removal and band ratioing.

Mahlei et al. (2013) described how each disease affects the leaf reflectance spectrum in a specific way. Therefore, an SDI should be developed based on the progression of disease symptoms and their spectral characteristics. Ashourloo et al. (2014) developed two SDIs on the basis of disease progression for detection of leaf rust in wheat. Most of the SDIs have been developed with a general interest to diagnose a plant disease at an early stage. As a matter of fact, different SDIs represent specificity, sensitivity and severity of the vegetation at different stages of infection. In general, a combination of red and NIR wavebands are used for the development of the vegetation index.

Clevers et al. (2004) and Broge and Leblanc (2001) reported that the common vegetation indices developed from combinations of red and NIR wavebands have also been useful for plant stress detection, such as Normalized Difference Vegetation Index (NDVI) (Rouse et al. 1974). For a very long time, NDVI has served as a plant stress indicator. However, recent studies conceptually differ from this notion. Most vegetation indices and spectral ratios provide information about a specific phenomenon only, such as crop vitality and greenness, which are not widely tested for disease diagnosis. Jimenez and Landgrebe (1999) reported that the selection of optimal wavebands for crop stress detection is very important. For development of SDI, wavebands must be free from redundant information without losing the ability for discrimination and class separability.

13.4.5 Unmanned Aerial Vehicle (UAV)

Over the years, the idea of developing vegetation indices has been popularized with the use of different airborne and satellite imageries. Processing airborne or satellite imageries is time consuming and very costly. Using an advanced hyperspectral camera onboard an UAV can be comparably more useful at the field scale. UAV allows for lower flight altitude and light-weight platform for hyperspectral camera. Recently, Behmann et al. (2018) described the disadvantage of not providing high-quality correction signals.

13.4.6 Geographic Information System (GIS) and Global Navigation Satellite System (GNSS)

For precision plant protection, GIS can play an important role in managing plant diseases in the field. A GIS usually needs GNSS coordinates, soil, crop, weather data and satellite imageries to serve as a decision support system. These data inputs are processed using several data analysis tools. Currently, GIS has emerged as a valuable tool to achieve the goal of precision plant protection. For plant disease management, GIS can be employed from field scale up to country scale. Remotely sensed vegetation indices with GIS can result in good outcomes for on-site plant disease assessment. GIS can provide an environment for utilizing the indices for studying crop health. For example, the application of NDVI data with phenological characteristics of plants can assess the suitability of remote sensing for estimating biotic and abiotic stress. This approach has become popular for analysis of phenological phenomena to facilitate disease detection, monitoring and diagnosis (Bolton and Friedl 2013; Chen et al. 2012; Granados-Ramírez et al. 2004). Damm et al. (2015) reported that NDVI along with photochemical reflectance index and sun-induced chlorophyll fluorescence can measure plant functional properties and detect infected vegetation canopies.

13.5 Machine Learning Techniques

13.5.1 Artificial Neural Network (ANN)

In recent years, there has been an increasing interest in applying ANN techniques for plant disease management. ANN techniques are capable of processing information similar to the way neurons process information in a human brain (Wasukar 2014). ANN requires a series of mathematical expressions, commonly referred to as algorithms. ANN is applicable for non-parametric regression, non-linear function, clustering, and data classification. Typically, ANN first analyzes the sample data and then makes a prediction from them (Paydipati 2004). Recently, Golhani et al. (2018) summarized relevant details of ANN mechanism, types, models, and classifiers in the context of plant disease detection using hyperspectral data. Basically, hyperspectral data provide near-continuous narrow-bands, which are helpful in developing spectral signatures and SDIs. The use of hyperspectral data has established ANN as an essential tool, particularly for large volume data processing. ANN has a powerful discriminating capability for plant disease classification, as it combines the best trainer sets for accurate classification (Golhani et al. 2018). For example, Zhu et al. (2016) processed the hyperspectral image for presymptomatic detection and classification of tobacco mosaic virus in tobacco leaves using back propagation neural network and PLS (see below).

13.5.2 Partial Least Square (PLS)

PLS is an extension of econometric path modeling which was developed during the late 1970s (Wold 1975). PLS was developed for solving chemometric problems, specifically for analyzing multivariate chemometric data (Martens 2001). Sundberg (1999) highlighted that PLS is appropriate for explaining a dependent factor where independent variables are also defined. Major advantages of PLS are the ability to reduce matrix dimensions, ability to find the number of relevant components, and ability to identify latent structure models in the data matrix (Helland 2001; Lingjaerde and Christophersen 2000). Therefore, PLS is known as a technique for analyzing spectroscopic data (Balabin and Smirnov 2011). PLS regression helps in obtaining stress sensitive wavebands from the VNIR spectrum. Van Maanen and Xu (2003) pointed out that an accurate regression model may reveal distinguished spectral patterns either before or after disease infection. Principally, PLS regression establishes the relationship between the independent variables (spectra) and the dependent variables (attribute information) (Indahl 2014). This method is superficially similar to principal component analysis where principal components are extracted from independent variables, and a regression model is established to predict the attribute information of unknown samples. PLS is often referred to as the analysis of multi co-linearity spectral data comprising a high degree of co-linearity among neighboring wavebands (Jones et al. 2010).

13.5.3 Cluster Analysis

Cluster analysis allows for grouping within spectral samples, also called dendrogram. A dendrogram is represented as a tree of spectral data which does not only identify similar groups of variables but successfully merges them (Ahmed et al. 2010; Iounousse et al. 2015). Krafft et al. (2009) explained that reflectance spectra are just like fingerprints which have different types of pattern. Cluster analysis works like a key to classify the pattern of fingerprints. In cluster analysis, the difference between subsets of clusters is minimized whereas the difference between groups of clusters is maximized. Lee et al. (2005) investigated a range of applications of cluster analysis for studying hardness and proximate constituents of maize kernel. They organized a total of 248 maize samples into 7 and 10 subgroups by cluster analysis. The groups resulting from cluster analysis had unique physical and chemical properties showing the different levels of hardness measurement. In a recent study, Golhani et al. (2017a) demonstrated the use of a spectroradiometer for reflectance measurement and cluster analysis to construct dendrograms of measured data. Their study was focused on a real-time screening of CCCVd-inoculated seedlings at the leaf scale.

13.6 Case Study of OS Detection

13.6.1 Experiment Details

13.6.1.1 Experiment Setup for Years 2015 and 2017

A research group comprising experts of precision agriculture, viroids and ANN has conducted a study to screen CCCVd-inoculated oil palm seedlings in a glass house. A highly infective CCCVd variant (OP₂₄₆) was used to inoculate three-months-old oil palm seedlings under a glasshouse facility in the Universiti Putra Malaysia (UPM), at Serdang, Selangor, Malaysia. Fifteen inoculated and ten healthy oil palm seedlings were evaluated throughout a 4-month experiment. The study was designed for two experimental years, 2015 and 2017. Reflectance data collected in the year of 2015 were used for calibration while data collected in 2017 were used for validation.

13.6.1.2 Reflectance Measurement at the Leaf Scale

The reflectance of inoculated and healthy seedlings were collected fortnightly from 15 through 120 days after inoculation (dai) using a spectroradiometer with hyper-spectral capacity. A VNIR range spectroradiometer (325–1075 nm), ASD FieldSpec-2, was used in 2015. While a full range spectroradiometer (350 nm–2500 nm), FieldSpec@4, was used in 2017. Spectroradiometers were employed at leaf scale using an ASD plant-probe containing a 100 W halogen reflectorized lamp. A 10 mm diameter portion of an oil palm leaf was clipped using the leaf-clip holder during spectral measurement. A total of twenty spectral readings were collected and averaged from each oil palm seedling.

13.6.1.3 SPAD Measurement

The chlorophyll content is a key indicator to assess the stress caused by OS disease in oil palm seedlings. Chlorophyll content was measured using a Minolta SPAD-502 (Konica Minolta, Inc. Japan), popularly known as SPAD meter, which measures chlorophyll content non-destructively at leaf scale within the range 0–100. The SPAD meter was used to measure chlorophyll content from the oil palm seedlings throughout the experiment. It measures a chlorophyll absorbance based on absorbance data collected at 650 nm and 940 nm (Castro and Sanchez-Azofeifa 2008). The chlorophyll content is measured in just a fraction of a second when a leaf is clamped between two Light Emitting Diodes (LEDs) positioned at the tip of the SPAD meter (Benetoli da Silva et al. 2012). The readings of chlorophyll content were taken between 10:00 am and noon, recording an average of five SPAD readings from the midrib of the third leaf of each seedling. SPAD readings were measured at an interval of 15 days through 120 dai.

13.7 Orange Spotting (OS) Detection

This case study was aimed at investigating reflectance data of Coconut cadang-cadang viroid (CCCVd)-inoculated seedlings at the VNIR region of the spectrum, especially at the red edge region (680–780 nm), located between the far red and the Near-infrared (NIR) wavelengths. The red edge region is able to extract precise and detailed information on crop stress. In the first step of this work, sensitive and insensitive wavebands were identified within the red edge region using cluster analysis. In the second step, the VNIR region was investigated using PLS for selecting the efficient wavebands, while four red edge indices were also evaluated using ANN. In the third and final step, the work generated a spectral index specifically for OS disease, i.e., OSDI by focusing on the red edge and twenty noble red edge parameters (Li et al. 2016). Details are given below.

13.7.1 Selection of Spectral Signature Using Cluster Analysis

Multivariate statistical techniques are widely applied to analyze hyperspectral remote sensing data. The application of hyperspectral data has been rapidly increasing thus far with the help of multivariate statistical technique such as cluster analysis. We used cluster analysis to extract the relevant spectral signature from reflectance of healthy and inoculated seedlings. This process typically involves identification of sensitive wavebands within the reflectance spectra, followed by determination of reflectance sensitivity.

Technically, cluster analysis produces groups of similar spectral reflectance. Similar reflectance spectra are closer to each other than dissimilar spectra. Joining these groups or clusters progressively results in a tree-like structure known as dendrogram. The scale at the top of the dendrogram is the normalized Euclidean distance among observations or clusters (Köksal 2011). By this process, reflectance spectra were archived from each interval of inoculation (i.e., days after inoculation, dai) of inoculated oil palm seedlings corresponding to 15, 30, 45 and 60 dai. At the same intervals, the reflectance of control seedlings was also collected. The dendrograms obtained from spectral readings of inoculated and healthy seedlings were used to compute the minimum Euclidean distance measured within each interval of spectral measurement. For example, Fig. 13.2a,b shows the dendrograms obtained from spectral readings of inoculated and healthy seedlings, measured at 30 dai, in which the nearest clusters based on minimum Euclidean distance were selected. Cluster A was found to be the nearest in both dendrograms. Its member spectra were averaged. As such, dendrograms of different inoculation intervals (15, 30, 45, 60 dai) were identified and their mean spectra were averaged to get the representative spectral signatures of inoculated and control oil palm seedlings (Fig. 13.3).

The representative spectra of inoculated and control seedlings were plotted against the VNIR region, specifically to understand changes in the red edge region.

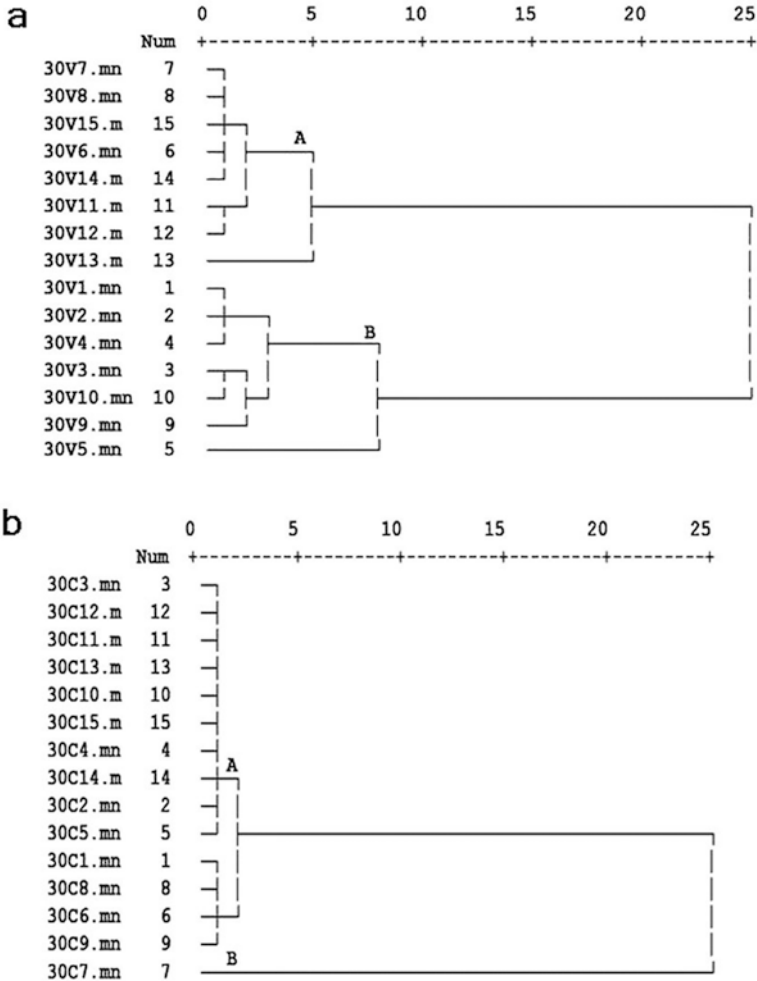


Fig. 13.2 Dendrogram structure of spectral reflectance obtained from fifteen inoculated (30 V1.mn – 30 V15.mn, **a**) and fifteen control seedlings (30C1.mn – 30C15.mn, **b**) at 30 days after inoculation

It was observed that the beginning point of red edge (680 nm), which is a relative chlorophyll absorption maxima, and a second point (754 nm), which is the first steep slope, were located in the red edge region (680–780 nm). This region has less reflectance due to chlorophyll absorption, while the NIR region is typically characterized by a high percentage of reflectance, due to the scattering of light in the intercellular mesophyll volume of leaves. Finally two spectral bands, 680 nm and 754 nm, were identified. A sharp change was also observed between 680 nm and 754 nm, which characterized a transition from chlorophyll absorption to leaf scattering in the red edge region.

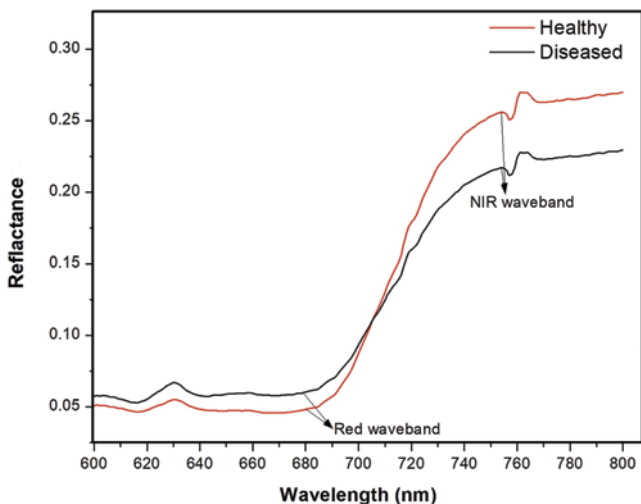


Fig. 13.3 Representative spectra of control and inoculated seedlings

Reflectance Sensitivity (RS), as proposed by Riedell et al. (2000), was applied to derive stress-sensitive and insensitive wavebands from these corresponding representative spectra (Fig. 13.3). As a result, an appreciable increase in RS (20%) was observed at 680 nm, while RS decreased up to 18% at 754 nm. To the authors' knowledge, these two red edge wavebands have not been previously studied for OS disease diagnosis in oil palm. These selected wavebands will be useful to screen infected seedlings prior to destructive sampling for biomolecular investigation. It is recommended that these wavebands be employed for evaluation of existing red edge indices and/or development of an SDI. This study provides a useful lead for canopy level diagnosis of OS disease in mature oil palm stands.

13.7.2 Estimating Chlorophyll Content Using PLS

The VNIR region (400–1050 nm) appears as most sensitive to chlorophyll stress. In this study, PLS regression was used to estimate chlorophyll content specifically from VNIR reflectance of CCCVd-inoculated and healthy oil palm seedlings. Information about chlorophyll stress could aid in diagnostics and decision-making for OS detection. Non-destructive estimation of chlorophyll content can be helpful in precision plant protection. In the PLS regression, independent and dependent variables need to be pre-defined before executing the program. For this, VNIR spectra were selected as independent variables and SPAD meter readings were selected as dependent variables. A Matlab freeware tool, Interval Partial Least-Squares Regression (iPLS), was used for estimating the chlorophyll content. Raw spectral data were pre-processed using first-order derivative, Savitzky-Golay (SG)

smoothing, Multiplicative Scatter Correction (MSC) and Standard Normal Transformation (SNV) methods.

Five datasets were prepared including the raw dataset. For each dataset, 80 samples were selected, in which 60 calibration samples were obtained from CCCVd-inoculated seedlings and 20 prediction samples were obtained from healthy oil palm seedlings. MSC pre-processed spectra gave outstanding performance with a root mean square error of prediction of 3.70% and a correlation coefficient for prediction of 0.72. Thirty sensitive wavebands (601–630 nm) were identified from VNIR reflectance using MSC pre-processed spectra. See technical and experimental details in Golhani et al. (2019b).

13.7.3 Selection of Red Edge Wavebands Using Artificial Neural Network (ANN)

A Multilayer Perceptron Neural Network (MLPNN) model was used to establish a relationship between red edge bands and spectral indices. Two spectral bands (700 nm and 768 nm) were identified from reflectance spectra of CCCVd-inoculated and healthy seedlings. The bands were used for evaluation of spectral indices, namely: simple ratio, red edge normalized difference vegetation index, two-band enhanced vegetation index 2 (EVI 2). In MLPNN model, identified spectral bands were used as input, and values of spectral indices were used as target. The EVI 2 resulted as best spectral index which resulted in zero errors at the training, testing, and validation datasets. In this work, the highest coefficient of correlation ($r = 1$) was recorded by EVI 2. Golhani et al. (2019a) mentioned that identified spectral bands and spectral index could be evaluated, using airborne or space-borne hyper-spectral sensor platforms, for detection of OS disease in mature oil palm stands.

13.7.4 Development of Orange Spotting Disease Index (OSDI)

The main purpose of this biennial experiment was to develop the OSDI, which could specifically be used for early detection of OS disease at the leaf scale. The OSDI was developed from reflectance spectra obtained from inoculated and healthy oil palm seedlings. It is believed that the OSDI values will give a reliable indication of OS disease, prior to confirmation by biomolecular marker techniques.

During the first experimental year (2015), twenty-four red edge parameters which were developed from First Derivative Reflectance (FDR) of the electromagnetic spectrum were used to develop the OSDI. Then, the OSDI values were verified with a repeated experiment in 2017. In Fig. 13.4, mean reflectance (30–120 dai) of diseased and healthy FDR was plotted in the red edge region. Four red edge parameters, viz. Red Edge Position (REP), mid-point (P), Right-side peak area (RSDR),

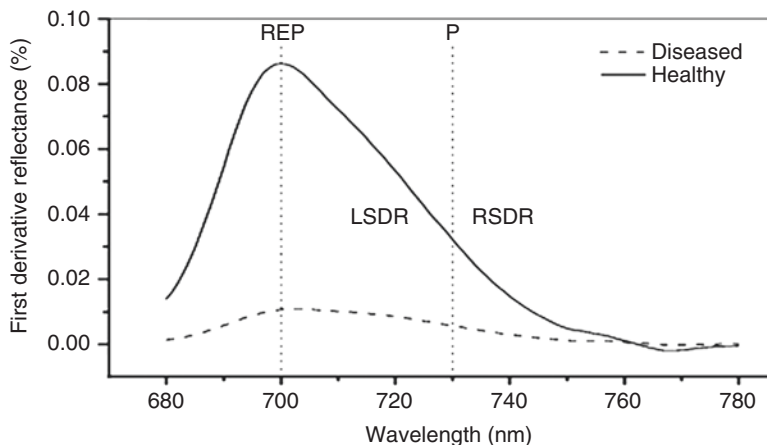


Fig. 13.4 A spectral plot of average spectra of healthy and diseased oil palm seedlings within the red edge region (680–780 nm) showing red edge parameters, viz. REP, LSDR, mid-point (P), and RSDR

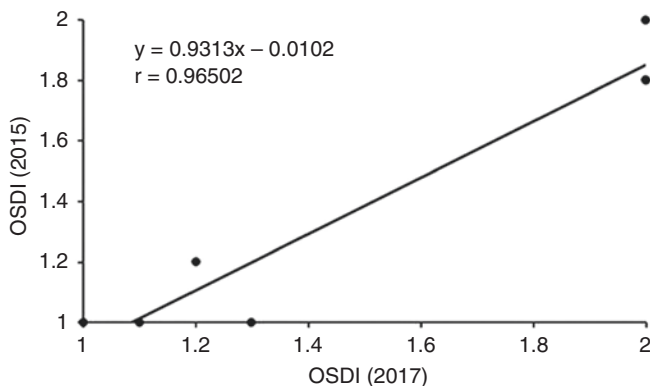


Fig. 13.5 Correlation between OSDI values computed in the years of 2015 and 2017

and Left-side peak area (LSDR), were studied to observe basic changes between diseased and healthy spectral signatures. In both spectra, reflectance increased in LSDR region between 680 nm and mid-point P nm, and decreased in RSDR region between P nm and 780 nm. REP was found at 700 nm, which could not be shifted towards shorter or longer wavelengths. This figure, while preliminary, suggested the need for exploration on other red edge parameters in order to find the most tangible criterion for comparison. Yang et al. (2010) mentioned that reflectance around the REP has been found to be most sensitive to plant stress.

Finally, a simple ratio representing the sum of the FDR of the right side – Red Edge Point (REP) to the sum of the FDR of the left side – REP of the red edge

region, was identified as OSDI. The validation results showed a strong correlation ($r = 0.96$) between OSDI values from experimental years of 2015 and 2017 (Fig. 13.5). In the future, OSDI values will be analyzed using ANN. OSDI is the first spectral index developed for detection of both symptomatic and asymptomatic OS-infected oil palms, at the leaf scale.

13.8 Conclusion

In this chapter, important drivers in precision agriculture have been discussed. A case study on OS detection was described. A precision approach to plant protection will expedite disease control and save financial resources and valuable time. In the shown case study, an attempt of quantifying reflectance data was made to augment effectiveness of OS phytopathometry appraisal in oil palm. Basically, CCCVd damages oil palm seedlings by crippling the chlorophyll apparatus. This case study showed that selected red edge wavebands, red edge indices, with the newly developed OSDI, are good predictors of chlorophyll stress caused by viroid attack. Development of the OSDI is the best outcome from this attempt, although to date, the newly developed OSDI has only been tested under a glasshouse environment. The verification of OSDI values under a wide range of growing conditions is recommended. Future work should be directed at investigating the efficacy of OSDI for diagnosis of OS disease at the canopy scale.

References

- Ahmed, S. S. S. J., Santosh, W., Kumar, S., & Thanka Christlet, T. H. (2010). Neural network algorithm for the early detection of Parkinson's disease from blood plasma by FTIR micro-spectroscopy. *Vibrational Spectroscopy*, 53, 181–188. <https://doi.org/10.1016/j.vibspec.2010.01.019>.
- Ashourloo, D., Mobasheri, M., & Huete, A. (2014). Developing two spectral disease indices for detection of wheat leaf rust (*Puccinia triticina*). *Remote Sensing*, 6, 4723–4740. <https://doi.org/10.3390/rs6064723>.
- Ashourloo, D., Matkan, A. A., Huete, A., Aghighi, H., & Mobasheri, M. R. (2016). Developing an index for detection and identification of disease stages. *IEEE Geosc Remote Sens Lett*, 13, 851–855. <https://doi.org/10.1109/LGRS.2016.2550529>.
- Ayala-Silva, T., & Beyl, C. A. (2005). Changes in spectral reflectance of wheat leaves in response to specific macronutrient deficiency. *Advances in Space Research*, 35, 305–317.
- Balabin, R. M., & Smimov, S. V. (2011). Variable selection in near-infrared spectroscopy: Benchmarking of feature selection methods on biodiesel data. *Analytica Chimica Acta*, 692, 63–72. <https://doi.org/10.1016/j.aca.2011.03.006>.
- Behmann, J., Acebron, K., Emin, D., Bennertz, S., Matsubara, S., Thomas, S., et al. (2018). Specim IQ: Evaluation of a new, miniaturized handheld hyperspectral camera and its application for plant phenotyping and disease detection. *Sensors*, 18, 441. <https://doi.org/10.3390/s18020441>.

- Beltrán-Peña, H., Soria-Ruiz, J., Téliz-Ortiz, D., Ochoa-Martínez, D. L., Nava-Díaz, C., & Ochoa-Ascencio, S. (2014). Molecular and satellite spectral imaging detection of Avocado Sunblotch Viroid (ASBVd). *Revista Fitotecnia Mexicana*, 37, 21–29.
- Benetoli da Silva, T. R., Reis de Sousa, A. C., & de Goés Maciel, C. D. (2012). Relationship between chlorophyll meter readings and total N in crambe leaves as affected by nitrogen topdressing. *Industrial Crops and Products*, 39, 135–138. <https://doi.org/10.1016/j.indcrop.2012.02.008>.
- Blackburn, G. A. (2007). Hyperspectral remote sensing of plant pigments. *Journal of Experimental Botany*, 58, 855–867. <https://doi.org/10.1093/jxb/erl123>.
- Blackmer, T. M., Schepers, J. S., & Meyer, G. E. (1995). Remote sensing to detect nitrogen deficiency in corn. In: *Site-specific management for agricultural systems* (pp. 505–512). <https://doi.org/10.2134/1995.site-specificmanagement.c35>.
- Bolton, D. K., & Friedl, M. A. (2013). Forecasting crop yield using remotely sensed vegetation indices and crop phenology metrics. *Agricultural and Forest Meteorology*, 173, 74–84. <https://doi.org/10.1016/j.agrformet.2013.01.007>.
- Broge, N. H., & Leblanc, E. (2001). Comparing prediction power and stability of broadband and hyperspectral vegetation indices for estimation of green leaf area index and canopy chlorophyll density. *Remote Sensing of Environment*, 76, 156–172. [https://doi.org/10.1016/S0034-4257\(00\)00197-8](https://doi.org/10.1016/S0034-4257(00)00197-8).
- Carter, G. A., & Knapp, A. K. (2001). Leaf optical properties in higher plants: Linking spectral characteristics to stress and chlorophyll concentration. *American Journal of Botany*, 88, 677. <https://doi.org/10.2307/2657068>.
- Carter, G. A., & Miller, R. L. (1994). Early detection of plant stress by digital imaging within narrow stress-sensitive wavebands. *Remote Sensing of Environment*, 50, 295–302. [https://doi.org/10.1016/0034-4257\(94\)90079-5](https://doi.org/10.1016/0034-4257(94)90079-5).
- Castro, K. L., & Sanchez-Azofeifa, G. A. (2008). Changes in spectral properties, chlorophyll content and internal mesophyll structure of senescing *Populus balsamifera* and *Populus tremuloides* leaves. *Sensors*, 8, 51–69. <https://doi.org/10.3390/s8010051>.
- Chaerle, L. (2004). Thermal and chlorophyll-fluorescence imaging distinguish plant-pathogen interactions at an early stage. *Plant & Cell Physiology*, 45, 887–896. <https://doi.org/10.1093/pcp/pch097>.
- Chappelle, E. W., Kim, M. S., & McMurtrey, J. E. (1992). Ratio analysis of reflectance spectra (RARS): An algorithm for the remote estimation of the concentrations of chlorophyll A, chlorophyll B, and carotenoids in soybean leaves. *Remote Sensing of Environment*, 39, 239–247. [https://doi.org/10.1016/0034-4257\(92\)90089-3](https://doi.org/10.1016/0034-4257(92)90089-3).
- Chen, X., Han, W., & Li, M. (2012). Spectroscopic determination of leaf water content using linear regression and an artificial neural network. *African Journal of Biotechnology*, 11, 2518–2527. <https://doi.org/10.5897/AJB11.2733>.
- Clevers, J. G. P. W., Kooistra, L., & Salas, E. A. L. (2004). Study of heavy metal contamination in river floodplains using the red-edge position in spectroscopic data. *International Journal of Remote Sensing*, 25, 3883–3895. <https://doi.org/10.1080/01431160310001654473>.
- Damm, A., Guanter, L., Verhoef, W., Schläpfer, D., Garbari, S., & Schaepman, M. E. (2015). Impact of varying irradiance on vegetation indices and chlorophyll fluorescence derived from spectroscopy data. *Remote Sensing of Environment*, 156, 202–215. <https://doi.org/10.1016/j.rse.2014.09.031>.
- Diener, T. O. (1999). Viroids and the nature of viroid diseases. In *100 Years of Virology* (pp. 203–220). Vienna: Springer. https://doi.org/10.1007/978-3-7091-6425-9_15.
- Gillespie, T. J., & Sentelhas, P. C. (2008). Agrometeorology and plant disease management: a happy marriage. *Science in Agriculture*. <https://doi.org/10.1590/S0103-90162008000700012>.
- Golhani, K., Balasundram, S. K., Vadamalai, G., & Pradhan, B. (2017a). Use of reflectance spectroscopy as a tool for screening viroid-inoculated oil palm seedlings. *Open Access Journal of Agricultural Research*, 2, 1–5. <https://doi.org/10.23880/OAJAR-16000145>.

- Golhani, K., Balasundram, S.K., Vadamalai, G., & Pradhan, B. (2017b). *Red-edge indices to diagnose orange spotting disease of oil palm in Malaysia*. In: 38th Asian Conference on Remote Sensing - Space Applications: Touching Human Lives, ACRS 2017.
- Golhani, K., Balasundram, S. K., Vadamalai, G., & Pradhan, B. (2018). A review of neural networks in plant disease detection using hyperspectral data. *Information Processing in Agriculture*, 5, 354–371. <https://doi.org/10.1016/j.inpa.2018.05.002>.
- Golhani, K., Balasundram, S. K., Vadamalai, G., & Pradhan, B. (2019a). Selection of a spectral index for detection of orange spotting disease in oil palm (*Elaeis guineensis* Jacq.) using red edge and neural network techniques. *Journal of the Indian Society of Remote Sensing*, 47, 639–646. <https://doi.org/10.1007/s12524-018-0926-4>.
- Golhani, K., Balasundram, S. K., Vadamalai, G., & Pradhan, B. (2019b). Estimating chlorophyll content at leaf scale in viroid- inoculated oil palm seedlings (*Elaeis guineensis* Jacq.) using reflectance spectra (400 nm–1050 nm). *International Journal of Remote Sensing*, 40, 647–7662. <https://doi.org/10.1080/01431161.2019.1584930>.
- Granados-Ramírez, R., Reyna-Trujillo, T., Gómez-Rodríguez, G., & Soria-Ruiz, J. (2004). Analysis of NOAA-AVHRR-NDVI images for crops monitoring. *International Journal of Remote Sensing*, 25, 1615–1627. <https://doi.org/10.1080/0143116031000156855>.
- Grinn-Gofroñ, A., Nowosad, J., Bosiacka, B., Camacho, I., Pashley, C., Belmonte, J., et al. (2019). Airborne *Alternaria* and *Cladosporium* fungal spores in Europe: forecasting possibilities and relationships with meteorological parameters. *Science of the Total Environment*, 653, 938–946.
- Grisham, M. P., Johnson, R. M., & Zimba, P. V. (2010). Detecting sugarcane yellow leaf virus infection in asymptomatic leaves with hyperspectral remote sensing and associated leaf pigment changes. *Journal of Virological Methods*, 167, 140–145. <https://doi.org/10.1016/j.jviromet.2010.03.024>.
- Helland, I. S. (2001). Some theoretical aspects of partial least squares regression. *Chemometrics and Intelligent Laboratory Systems*, 58, 97–107. [https://doi.org/10.1016/S0169-7439\(01\)00154-X](https://doi.org/10.1016/S0169-7439(01)00154-X).
- Huete, A. R. (1989). Soil influences in remotely sensed vegetation-canopy spectra. In G. Asrar (Ed.), *Theory and applications of optical remote sensing* (pp. 107–141). New York: Wiley-Interscience.
- Indahl, U. G. (2014). The geometry of PLS1 explained properly: 10 key notes on mathematical properties of and some alternative algorithmic approaches to PLS1 modelling. *Journal of Chemometrics*, 28, 168–180. <https://doi.org/10.1002/cem.2589>.
- Iounousse, J., Er-Raki, S., El Motassadeq, A., & Chehouani, H. (2015). Using an unsupervised approach of Probabilistic Neural Network (PNN) for land use classification from multitemporal satellite images. *Applied Soft Computing*, 30, 1–13. <https://doi.org/10.1016/j.asoc.2015.01.037>.
- Jimenez, L. O., & Landgrebe, D. A. (1999). Hyperspectral data analysis and supervised feature reduction via projection pursuit. *IEEE Transactions on Geoscience and Remote Sensing*, 37, 2653–2667.
- Jones, C. D., Jones, J. B., & Lee, W. S. (2010). Diagnosis of bacterial spot of tomato using spectral signatures. *Computers and Electronics in Agriculture*, 74, 329–335. <https://doi.org/10.1016/j.compag.2010.09.008>.
- Knipling, E. B. (1970). Physical and physiological basis for the reflectance of visible and near-infrared radiation from vegetation. *Remote Sensing of Environment*, 1, 155–159. [https://doi.org/10.1016/S0034-4257\(70\)80021-9](https://doi.org/10.1016/S0034-4257(70)80021-9).
- Köksal, E. S. (2011). Hyperspectral reflectance data processing through cluster and PCA for estimating irrigation and yield related indicators. *Agricultural Water Management*, 98, 1317–1328. <https://doi.org/10.1016/j.agwat.2011.03.014>.
- Krafft, C., Steiner, G., Beleites, C., & Salzer, R. (2009). Disease recognition by infrared and Raman spectroscopy. *Journal of Biophotonics*, 2, 13–28. <https://doi.org/10.1002/jbio.200810024>.
- Krezhova, D., Stoev, A., & Maneva, S. (2015). Detection of biotic stress caused by apple stem grooving virus in apple trees using hyperspectral reflectance analysis. *Comptes Rendus de l'Académie Bulgare des Sciences*, 68, 175–182.
- Kuska, M. T., & Mahlein, A. K. (2018). Aiming at decision making in plant disease protection and phenotyping by the use of optical sensors. *The European Journal of Plant Pathology*, 1–6.

- Lacis, A. A., & Hansen, J. (1974). A parameterization for the absorption of solar radiation in the earth's atmosphere. *Journal of the Atmospheric Sciences*, *31*, 118–133.
- Lee, K. M., Herrman, T. J., Lingenfelter, J., & Jackson, D. S. (2005). Classification and prediction of maize hardness-associated properties using multivariate statistical analyses. *Journal of Cereal Science*, *41*, 85–93. <https://doi.org/10.1016/j.jcs.2004.09.006>.
- Lee, W. S., Alchanatis, V., Yang, C., Hirafuji, M., Moshou, D., & Li, C. (2010). Sensing technologies for precision specialty crop production. *Computers and Electronics in Agriculture*, *74*, 2–33. <https://doi.org/10.1016/j.compag.2010.08.005>.
- Lemon, S. M., Hamburg, M. A., Sparling, P. F., Choffnes, E. R., & Mack, A. (2007). *Global infectious disease surveillance and detection : assessing the challenges — finding solutions*. Workshops summary (p. 284). Washington, DC: National Academies Press. doi:978-0-309-11114-0.
- Li, L., Ustin, S. L., & Lay, M. (2005). Application of AVIRIS data in detection of oil-induced vegetation stress and cover change at Jornada, New Mexico. *Remote Sensing of Environment*, *94*, 1–16. <https://doi.org/10.1016/j.rse.2004.08.010>.
- Li, L., Ren, T., Ma, Y., Wei, Q., Wang, S., Li, X., et al. (2016). Evaluating chlorophyll density in winter oilseed rape (*Brassica napus* L.) using canopy hyperspectral red-edge parameters. *Computers and Electronics in Agriculture*, *126*, 21–31. <https://doi.org/10.1016/j.compag.2016.05.008>.
- Lingjaerde, O. C., & Christophersen, N. (2000). Shrinkage structure of partial least squares. *Scandinavian Journal of Statistics*, *27*, 459–473. <https://doi.org/10.1111/1467-9469.00201>.
- Mahlei, A.-K., Rumpf, T., Welke, P., Dehne, H.-W., Plümer, L., Steiner, U., & Oerke, E.-C. (2013). Development of spectral indices for detecting and identifying plant diseases. *Remote Sensing of Environment*, *128*, 21–30. <https://doi.org/10.1016/j.rse.2012.09.019>.
- Mahlein, A. (2010). *Detection, identification and quantification of fungal diseases of sugar beet leaves using imaging and non-imaging hyperspectral techniques*. Bonn: University of Bonn.
- Mahlein, A. K. (2016). Plant disease detection by imaging sensors – parallels and specific demands for precision agriculture and plant phenotyping. *Plant Disease*, *100*, 241–251. <https://doi.org/10.1094/PDIS-03-15-0340-FE>.
- Martens, H. (2001). Reliable and relevant modelling of real world data: a personal account of the development of PLS regression. *Chemometrics and Intelligent Laboratory Systems*, *58*, 85–95.
- Martinelli, F., Scalenghe, R., Davino, S., Panno, S., Scuderi, G., Ruisi, P., et al. (2014). Advanced methods of plant disease detection. A review. *Agronomy for Sustainable Development*, *35*, 1–25. <https://doi.org/10.1007/s13593-014-0246-1>.
- Merzlyak, M. N., Gitelson, A. A., Chivkunova, O. B., Solovchenko, A. E., & Pogosyan, S. I. (2003). Application of reflectance spectroscopy for analysis of higher plant pigments. *Russian Journal of Plant Physiology*, *50*, 704–710.
- Oerke, E. C., Gerhards, R., Menz, G., & Sikora, R. A. (2010). *Precision crop protection-the challenge and use of heterogeneity* (p. 441). Dordrecht: Springer.
- Paydipati, R. (2004). Evaluation of classifiers for automatic disease detection in citrus leaves machine vision. Master Thesis, Univ. FL. In USA.
- Pinter, P. J., Hatfield, J. L., Schepers, J. S., Barnes, E. M., Moran, M. S., Daughtry, C. S. T., & Upchurch, D. R. (2003). Remote sensing for crop management. *Photogrammetric Engineering and Remote Sensing*, *69*, 647–664. <https://doi.org/10.14358/PERS.69.6.647>.
- Riedell, W.E., Osborne, S.L., Hesler L.S., & Blackmer, T.M. (2000). Remote sensing of insect damage in wheat. In: *Proceedings of the 5th International Conference on Precision Agriculture, Bloomington, Minnesota, USA* (16–19 July, 2000), 1–11.
- Rouse, J. W., Haas, R. H., Deering, D. W., & Harlan, J. C. (1974). *Monitoring the vernal advancement and retrogradation (green wave effect) of natural vegetation*. Greenbelt: NASA/GSFC type III final report.
- Rumpf, T., Mahlein, A., Dörschlag, D., & Plümer, L. (2009). Identification of combined vegetation indices for the early detection of plant diseases. In: C.M.U. Neale, and A. Maltese (Eds.). *SPIE Europe Remote Sensing*, 747217. doi:<https://doi.org/10.1117/12.830525>.

- Rumpf, T., Mahlein, A.-K., Steiner, U., Oerke, E.-C., Dehne, H.-W., & Plümer, L. (2010). Early detection and classification of plant diseases with support vector machines based on hyperspectral reflectance. *Computers and Electronics in Agriculture*, *74*, 91–99. <https://doi.org/10.1016/j.compag.2010.06.009>.
- Schellber, J., Hill, M. J., Gerhards, R., Rothmund, M., & Braun, M. (2008). Precision agriculture on grassland: applications, perspectives and constraints. *European Journal of Agronomy*, *29*, 59–71.
- Selvaraja, S., Balasundram, S. K., Vadamalai, G., & Husni, M. H. A. (2013). Site-specific disease management: a preliminary case with orange spotting in oil palm. In J. V. Stafford (Ed.), *Precision Agriculture '13*. Wageningen Academic Publishers. https://doi.org/10.3920/978-90-8686-778-3_71.
- Slonecker, E. (2011). Analysis of the effects of heavy metals on vegetation hyperspectral reflectance properties. In *Hyperspectral remote sensing of vegetation* (pp. 561–578). Boca Raton: CRC Press. <https://doi.org/10.1201/b11222-33>.
- Steele, M., Gitelson, A. A., & Rundquist, D. (2008). Nondestructive estimation of leaf chlorophyll content in grapes. *American Journal of Enology and Viticulture*, *2*, 299–305. <https://doi.org/10.2307/2445170>.
- Sundberg, R. (1999). Multivariate calibration — direct and indirect regression methodology. *Scandinavian Journal of Statistics*, *26*, 161–207.
- Thanarajoo, S. S. (2014). *Rapid detection, accumulation and translocation of Coconut cadang-cadang viroid variants in oil palm*. Serdang: Universiti Putra Malaysia.
- Thomas, S., Wahabzada, M., Kuska, M. T., Rascher, U., & Mahlein, A. K. (2017). Observation of plant–pathogen interaction by simultaneous hyperspectral imaging reflection and transmission measurements. *Functional Plant Biology*, *44*, 23–34.
- Thomas, S., Kuska, M. T., Bohnenkamp, D., Brugger, A., Alisaac, E., Wahabzada, M., et al. (2018). Benefits of hyperspectral imaging for plant disease detection and plant protection: A technical perspective. *The Journal of Plant Diseases and Protection*, *125*, 5–20.
- Vadamalai, G., Hanold, D., Rezaian, M. A., & Randles, J. W. (2006). Variants of Coconut cadang-cadang viroid isolated from an African oil palm (*Elaeis guineensis* Jacq.) in Malaysia. *Archives of Virology*, *151*, 1447–1456. <https://doi.org/10.1007/s00705-005-0710-y>.
- Van Maanen, A., & Xu, X. M. (2003). Modelling plant disease epidemics. In *Epidemiology of Mycotoxin Producing Fungi* (pp. 669–682). Dordrecht: Springer. https://doi.org/10.1007/978-94-017-1452-5_2.
- Wasukar, A. R. (2014). Artificial neural network – an important asset for future computing. *International Journal of Emerging Trends in Science*, *1*, 28–34.
- West, J. S., Bravo, C., Oberti, R., Moshou, D., Ramon, H., & McCartney, H. A. (2010). Detection of fungal diseases optically and pathogen inoculum by air sampling. In *Precision crop protection - the challenge and use of heterogeneity* (pp. 135–149). Dordrecht: Springer. https://doi.org/10.1007/978-90-481-9277-9_9.
- Wold, H. (1975). Soft modeling by latent variables: the nonlinear iterative partial least squares (NIPALS) approach. *Journal of Applied Probability*, *12*(S1), 117–142.
- Wu, Y. H., Cheong, L. C., Meon, S., Lau, W. H., Kong, L. L., Joseph, H., & Vadamalai, G. (2013). Characterization of Coconut cadang-cadang viroid variants from oil palm affected by orange spotting disease in Malaysia. *Archives of Virology*, *158*, 1407–1410. <https://doi.org/10.1007/s00705-013-1624-8>.
- Yang, F., Li, J., Gan, X., Qian, Y., Wu, X., & Yang, Q. (2010). Assessing nutritional status of *Festuca arundinacea* by monitoring photosynthetic pigments from hyperspectral data. *Computers and Electronics in Agriculture*, *70*, 52–59. <https://doi.org/10.1016/j.compag.2009.08.010>.
- Zhao, X. (2012). Advances and technology in infrared spectroscopy. *Journal of Anqing Teachers College*, *18*, 94–97.
- Zhu, H., Cen, H., Zhang, C., & He, Y. (2016). Early detection and classification of tobacco leaves inoculated with tobacco mosaic virus based on hyperspectral imaging technique. *ASABE Annual International Meeting*, *1*. <https://doi.org/10.13031/aim.20162460422>.